X-ray Powder Diffraction and Solid-State NMR Investigations in Cadmium−Lead Hydroxyapatites

Béchir Badraoui,[a] Adriana Bigi,*[b] Mongi Debbabi,[a] Massimo Gazzano,[c] Norberto Roveri,[b] and René Thouvenot[d]

Dedicated to Professor Alberto Ripamonti on the occasion of his 70th birthday

Keywords: Hydroxyapatite / Rietveld method / ^{31}P MAS NMR spectroscopy / Ionic substitution / X-ray diffraction

In the proposed experiment, the maximum amount of cadmium substitution in lead hydroxyapatite accounts for about 30 atom-%. The crystal structures of PbHA at different degrees of cadmium substitution for lead (4.9, 10.0, 22.4 and 29.0% Cd atoms) have been investigated by X-ray powder pattern fitting and ^{31}P MAS NMR. The site-occupancy factors of metal atoms clearly indicate a preference of cadmium for site **1** of the apatite structure, which is more selective at low cadmium content. A progressive shift of the OH group towards the center of the triangles formed by the site **2** metals has been observed with increasing cadmium content. The different environments of the phosphate group demonstrated by ^{31}P NMR spectroscopic data are discussed in relation to structural data.

Introduction

Hydroxyapatite (CaHA), $Ca_{10}(PO_4)_6(OH)_2$, is a member of a large family of isomorphous substances, and the study of its physico-chemical properties represents an area of intensive interdisciplinary research activity. CaHA is of great interest in the design of biomaterials, in chromatography, in catalysis and in water treatment.[1,2] The CaHA structure can easily host a variety of substituents, both cationic and anionic, whose presence affects the physico-chemical properties of the compound.[3−7] Ionic substitutions can be involved in several applications: dental and bone pathologies, pollution due to phosphate fertilizers, ion-exchange properties for water treatment, radioactive waste confinement, bioceramics for bone implants, catalysis, luminescence, phosphorescence, etc. The most frequently encountered form of CaHA crystallizes in the hexagonal $P6_3/m$ space group, with lattice constants a = 9.42 Å and c = 6.88 Å.[2] The unit cell contains ten cations arranged in two nonequivalent sites: four at site **1** and six at site **2**, as shown in Figure 1. At site **1**, Ca ions are aligned in columns and surrounded by nine oxygen atoms. Ca ions at site **2** are arranged in equilateral triangles centered on the screw axes and surrounded by seven oxygen atoms, one of which belongs to the OH^- groups and the others to the PO_4^{3-} tetrahedra. The OH^- groups occur in columns parallel to the c axis and pass through the centers of the calcium triangles. Among the divalent cations which can be incorporated into the CaHA structure, cadmium, strontium and lead are known to replace calcium in the whole range of composition, while barium−calcium hydroxyapatite exhibits a zone of immiscibility.[8−12] The lattice parameters of these mixed apatites vary linearly with the composition, with the exception of the c axis of lead−calcium hydroxyapatite that displays a discontinuity at about 50 atom-% of lead. The peculiar variation of the c-axis dimension has been ascribed to an inhomogeneous lead distribution at the two nonequivalent cation sites, on the basis of the results of powder pattern structure refinements of Pb−Ca apatites, which indicate a clear preference of lead for site **2** of the hydroxyapatite structure.[9]

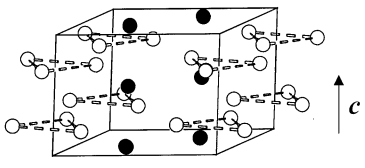

Figure 1. Perspective view of the metal ion in site **1** (black circles) and site **2** (white circles) of HA structure

We now report the results of an X-ray powder pattern fitting study and of a ^{31}P NMR investigation carried out on Cd−Pb mixed hydroxyapatite samples prepared from solutions containing 5 (Cd5), 10 (Cd10), 20 (Cd20) and 30

[a] Laboratoire de Chimie Inorganique et Industrielle, Ecole Nationale d'Ingénieurs de Monastir,
5019 Monastir, Tunisie
[b] Dipartimento di Chimica "G. Ciamician", Università degli Studi,
Via Selmi 2, 40126 Bologna, Italy
Fax: (internat.) + 39-051/209-9456
E-mail: bigi@ciam.unibo.it
[c] Centro di Studio per la Fisica delle Macromolecole, C.N.R.,
Via Selmi 2, 40126 Bologna, Italy
[d] Laboratoire de Chimie Inorganique et Matériaux Moléculaires, Unité CNRS 7071, case courrier 42, Université Pierre et Marie Curie,
75252 Paris Cedex 05, France
Supporting information for this article is available on the WWW under http://www.wiley-vch.de/home/eurjic or from the author.

  1434−1948/01/0505−1261 $ 17.50+.50/0

(Cd30) atom-% Cd. The results give important details of the structural modifications induced by cadmium on the lead hydroxyapatite structure.

Results

The results of the structural refinements indicate that the maximum amount of cadmium substitution in lead hydroxyapatite (PbHA; hereafter MHA = metal apatite) accounts for about 30 atom-%. In other words, the upper limit of the solid solutions is $Cd_3Pb_7(PO_4)_6(OH)_2$. In spite of the limited range of Cd incorporation, the decrease in cell parameters is quite regular when the amount of Cd increases, indicating true solid solutions and a behavior according to Vegard's law, where x = Cd × 100/(Cd + Pb) and σ values are the standard deviation:

$a = (9.8765 - 0.0062\ x)$, $\sigma(a) = 1.3 \times 10^{-4}$ Å
$c = (7.4148 - 0.0080\ x)$, $\sigma(c) = 2.4 \times 10^{-4}$ Å

Increasing amounts of CdO are present in the preparations obtained at greater Cd concentrations, up to 60%. At even greater concentrations [i.e. Cd/(Cd + Pb) > 60%], the products display nonapatitic powder X-ray diffraction patterns, characteristic of lead-substituted tricadmium phosphate.

Table 1. Fractional atomic coordinates after Rietveld refinement for the mixed Cd−Pb hydroxyapatites (e.s.d. in parentheses)

Sample	Atom	x	y	z
Cd5[a]	M(1)	0.3333	0.6666	−0.0010(15)
	M(2)	0.2505(4)	1.0038(7)	0.2500
	P	0.394(2)	0.353(2)	0.2500
	O(1)	0.344(3)	0.491(3)	0.2500
	O(2)	0.567(4)	0.482(3)	0.2500
	O(3)	0.323(3)	0.247(2)	0.082(3)
	OH	0.0000	0.0000	0.080(4)
Cd10[b]	M(1)	0.3333	0.6666	0.0021(8)
	M(2)	0.2495(3)	1.0022(6)	0.2500
	P	0.399(1)	0.363(1)	0.2500
	O(1)	0.347(3)	0.482(2)	0.2500
	O(2)	0.577(3)	0.471(3)	0.2500
	O(3)	0.326(2)	0.254(2)	0.083(2)
	OH	0.0000	0.0000	0.120(2)
Cd20[c]	M(1)	0.3333	0.6666	0.0043(2)
	M(2)	0.2480(4)	0.9990(6)	0.2500
	P	0.408(1)	0.380(2)	0.2500
	O(1)	0.349(2)	0.501(3)	0.2500
	O(2)	0.593(3)	0.454(3)	0.2500
	O(3)	0.354(2)	0.285(2)	0.085(2)
	OH	0.0000	0.0000	0.167(5)
Cd30[d]	M(1)	0.3333	0.6666	0.0108(2)
	M(2)	0.2517(5)	1.0005(9)	0.2500
	P	0.413(2)	0.389(3)	0.2500
	O(1)	0.331(4)	0.482(3)	0.2500
	O(2)	0.609(3)	0.473(4)	0.2500
	O(3)	0.346(2)	0.282(3)	0.092(3)
	OH	0.0000	0.0000	0.163(5)

[a] a = 9.861(1) Å, c = 7.3604(1) Å, R_p = 7.8, R_{wp} = 10.1. − [b] a = 9.810(1) Å, c = 7.3315(6) Å, R_p = 5.5, R_{wp} = 7.3. − [c] a = 9.741(1) Å, c = 7.2522(7) Å, R_p = 6.5, R_{wp} = 8.3. − [d] a = 9.692(1) Å, c = 7.174(1) Å, R_p = 10.5, R_{wp} = 13.5.
The pattern R factor R_p is defined as $R_p = 100\{\Sigma|Y_{oi} - Y_{ci}|/\Sigma Y_{oi}\}$. The weighted pattern R factor R_{wp} is defined as $R_{wp} = 100\{\Sigma w_i(Y_{oi} - Y_{ci})^2/\Sigma w_i(Y_{oi})^2\}^{1/2}$.

X-ray Data

The refined structural parameters of the samples Cd5, Cd10, Cd20 and Cd30 are reported in Table 1, and the data about cationic distribution are reported in Table 2. Figure 2 displays the final plot for Cd10 sample as a typical comparison between the observed and calculated profiles. The final agreement indices, R_{wp}, are 10.1, 7.3, 8.3 and 13.5 for Cd5, Cd10, Cd20 and Cd30, respectively. The bond lengths and angles for the two metal environments are reported in Table 3.

The refinement of the four samples of Cd−PbHA indicates that the cadmium content in the crystalline phase of these samples is 8.4, 10.0, 22.4 and 29.0 for Cd5, Cd10, Cd20 and Cd30, respectively. These values are very close to those expected on the basis of the stoichiometry of the reagents and on chemical analysis (4.9, 10.6, 21.0 and 30.6, respectively), with the exception of Cd5, which exhibits an appreciably greater Cd incorporation.

^{31}P NMR Spectroscopic Data

The 162 MHz ^{31}P MAS spectra of Cd5 and Cd30 are presented in Figure 3 and the relevant data are reported on Table 4. Two distinct isotropic signals can be detected for the two low cadmium containing apatites but only a relatively broad band occurs for Cd20 and Cd30.

Discussion

Structural Analysis

Cadmium can replace lead in the hydroxyapatite structure by up to about 30 atom-%, inducing a linear contraction of the lattice constants in agreement with its smaller size. The partial miscibility found for Cd−Pb apatites is in contrast with the behaviour observed for Cd−Ca and Pb−Ca apatites.[6,13] The complete miscibility of Ca and Cd hydroxyapatites is not surprising in view of their similar size, which is not the case for Ca and Pb ions. The miscibility of the Ca−Pb hydroxyapatites can be justified on the basis of the large difference in the polarizabilities of calcium and lead ions: Ca^{2+} is a hard acid, giving mainly ionic interactions with oxygen, whereas Pb^{2+} is a soft acid, displaying a considerable tendency towards polarization and covalent interactions. In the Cd−Pb case, we have two soft acids. Their significant tendency towards covalent interactions and directional bonding, which is most likely the origin of the large distortions of the PO_4 tetrahedra, probably limits the possibility of mutual substitution. In particular, the precipitation of nonapatitic phases at high cadmium concentrations suggests that the presence of lead, even in small amounts, inhibits the formation of CdHA.

The results of the powder fitting structure refinements indicate a clear preference of cadmium for site **1** of the apat-

Table 2. Cadmium substitution (atom-%) in Cd−Pb hydroxyapatites, e.s.d. in parentheses

	Cd1/(Cd1 + Pb1)	Cd1/(Cd1 + Cd2)	Cd2/(Cd1 + Cd2)	Cd2/(Cd2 + Pb2)	Cd/(Cd + Pb)[a]
Cd5	21(1)	99(1)	1(1)	<1	8.4(4)
Cd10	23(1)	92(1)	8(1)	1.3(2)	10.0(5)
Cd20	44(2)	79(1)	21(1)	8.0(4)	22.4(9)
Cd30	49(3)	67(2)	33(2)	16(2)	29(2)

[a] Cd = Cd1 + Cd2, Pb = Pb1 + Pb2.

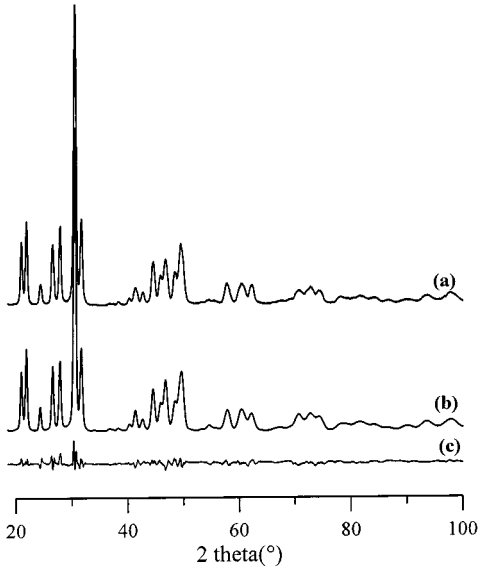

Figure 2. Observed (a) and calculated (b) XRD patterns of the sample Cd10; the curve difference is (c)

Table 3. Environments of metal atoms in Cd−Pb hydroxyapatites, e.s.d. in parentheses

	PbHA[12]	Cd5	Cd10	Cd20	Cd30	CdHA[11]
M(1)−O(1) × 3	2.67(2)	2.57(2)	2.62(2)	2.46(2)	2.47(2)	2.326(7)
M(1)−O(2) × 3	2.54(2)	2.81(4)	2.69(3)	2.48(3)	2.53(3)	2.437(8)
M(1)−O(3) × 3	3.00(2)	3.11(2)	3.09(2)	2.92(2)	2.98(3)	2.826(9)
M(1)−O mean	*2.73*	*2.83*	*2.80*	*2.62*	*2.66*	*2.530*
M(2)−O(1)	2.89(2)	3.05(3)	3.03(2)	3.03(3)	2.85(3)	2.636(9)
M(2)−O(2)	2.54(2)	2.34(2)	2.39(2)	2.51(2)	2.31(3)	2.354(9)
M(2)−O(3) × 2	2.59(1)	2.57(2)	2.51(2)	2.59(2)	2.58(3)	2.487(9)
M(2)−O(3) × 2	2.62(1)	2.45(2)	2.56(2)	2.75(2)	2.66(3)	2.241(7)
M(2)−OH	2.89(2)	2.75(1)	2.616(7)	2.49(2)	2.51(1)	2.351(3)
M(2)−O mean	*2.68*	*2.60*	*2.59*	*2.60*	*2.59*	*2.466*
M(2)−M(2)	4.22(1)	4.422(6)	4.402(5)	4.193(6)	4.221(7)	4.008(1)
M(2)−M(1)	4.19(1)	4.225(6)	4.185(6)	4.128(7)	4.074(8)	3.896(1)
M(1)−M(1)	3.62(2)	3.666(6)	3.697(6)	3.564(6)	3.432(9)	3.288(1)

ite structure. At low concentrations, Cd occupies almost exclusively site **1**, whereas at a higher degree of substitution, the selectivity is smaller, although the preference is maintained. As is clearly shown in Table 2, most of the Cd ions in Cd5 (99%) are at site **1**. The occupancy of site **1** by Cd decreases to 92% in Cd10, to 79% in Cd20 and to 67% in Cd30, in which about 50% of the metal atoms at site **1** are Cd. This result could be expected on the basis of the shorter metal−metal distances at site **1** (M−M = 3.62 Å in PbHA) which is more suitable for the smaller Cd ion, than at site **2** (M−M = 4.22 Å in PbHA). Furthermore, this is in agreement with the preference of Pb for site **2**, where the arrangement of the "staggered" equilateral triangles allows for the optimization of the packing of larger ions, in contrast to site **1** where the strict alignment of the columns causes a stronger repulsion.

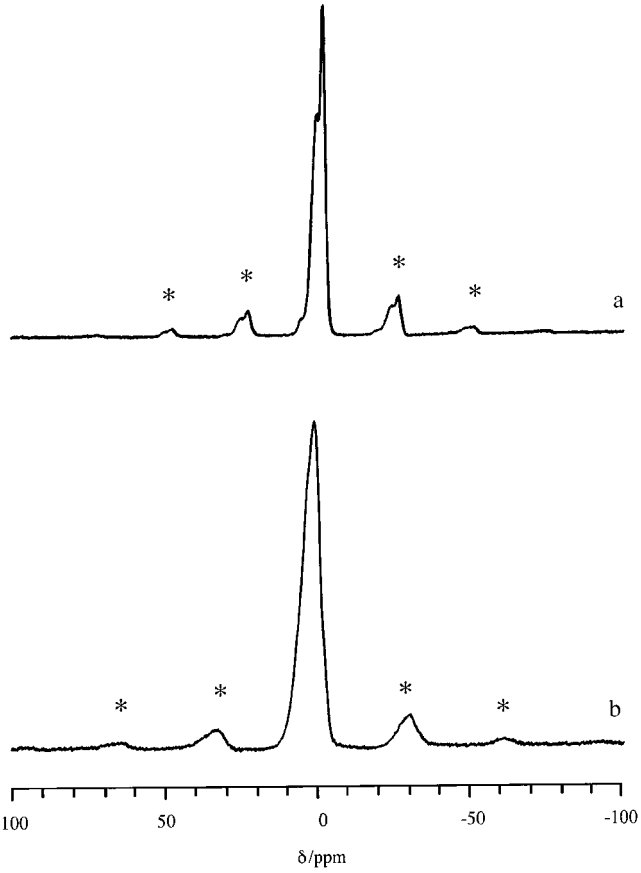

Figure 3. 162 MHz ^{31}P MAS NMR spectra of (a) Cd5 (spinning rate 4 kHz) and (b) Cd30 (spinning rate 5 kHz); asterisks mark spinning side bands

Table 4. ^{31}P MAS solid-state NMR spectroscopic data

Sample	δ_{iso} (ppm)	$\Delta\nu_{1/2}$ [a]	Relative amount[b] (%)
Cd5	−1.1	1.9 (310)[b]	47
	+0.9	3.1 (500)[b]	53
Cd10	−1.0	1.6 (260)[b]	27
	+1.1	4.3 (700)[b]	73
Cd20	+1.8	5.3 (860)	−
Cd30	+1.9	7.0 (1130)	−

[a] In ppm, with the values in Hz in parentheses. − [b] From line-fitting analysis.

For the sample Cd5, the discrepancy between the value of the cadmium content obtained from the Rietveld refinement and the value measured by chemical analysis, can be ascribed to the slight modification of the diffraction pattern induced by cadmium incorporation: 5% of lead substituted by cadmium corresponds to only a 1.5% intensity variation in the region of the most intense peaks (ca. 30° − 2θ). Furthermore, the value of the Cd5 unit-cell volume is an indirect confirmation that cadmium substitution amounts to approximately 5%, since it fits very well with those of the other samples in the plot of volume against Cd%.

The insertion of cadmium into the PbHA lattice appreciably affects the position of the OH group in the channel formed by the metals of site **2**, as can be seen in Figure 3. In CdHA, as well as in CaHA, the OH ion is just a little bit out of the plane of the triangles formed by the site **2** metals; on the other hand, the OH ion in PbHA is approximately halfway between two successive planes of lead triangles, because of the presence of the larger metal ions. The substitution of cadmium for lead causes a shift of the group along the channel toward the center of the plane (see Figure 4) with a behaviour very similar to that previously verified for Pb−Ca hydroxyapatite.[9] The shift is also appreciable when a very small amount of cadmium is inserted at site **2**, as reported in Table 3 for Cd5 and Cd10.

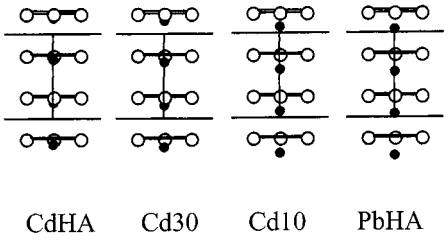

Figure 4. A view of the OH oxygen position (black circles) along the *z* axis in CdHA, PbHA and mixed Cd−Pb hydroxyapatites

The distortion indices of the phosphate group of the solid solutions (data are reported in the Supporting Information) are greater than those of the end members, indicating that the cationic substitution also induces deformations in the phosphate tetrahedra. In any case, the observed distorsions are consistent with the data reviewed by Baur.[14]

Cd−PbHA ^{31}P MAS NMR

The pure phases, $Cd_{10}(PO_4)_6(OH)_2$ and $Pb_{10}(PO_4)_6(OH)_2$, each present a unique isotropic signal at $\delta = +12.2$ and -0.7, respectively, according to the presence of a unique crystallographic site for the phosphate group in the apatitic cell. The chemical shift variation between CdHA and PbHA can be correlated to the increase in the lattice parameters.[15]

It should be noted that the chemical shift difference between these two phases is relatively large ($\Delta\delta \approx 13$), because the signal for CdHA is the most deshielded of the known hydroxyapatites for which δ_{iso} is in the range -0.7 to $+2.9$.[16−18] When considering the partial substitution of Cd for Pb at the metallic sites, one has to consider the cationic environment of the phosphate group. The phosphorous atom displays 9 (O−M) contacts, as shown in Figure 5.

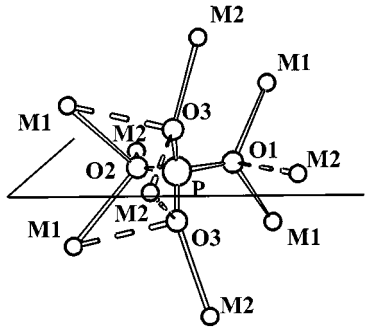

Figure 5. The cationic environment of the phosphate group; the bonds longer than 2.7 Å are dotted; the mirror plane is enhanced

If we assume a statistical distribution of the cadmium atoms over the different sites, one would expect, through progressive replacement of Pb by Cd, various cationic environments, ranging from zero cadmium, nine lead atoms (abbreviated as PPb_9) to nine cadmium, zero lead atoms (abbreviated as PCd_9). In the frame of this assumption, the relative proportion of a $PCd_xPb_{(9-x)}$ environment (x = integer) is given by the statistical formula

$$p_{[PCd_xPb_{9-x}]} = C_9^x\, p_{Cd}^x\, p_{Pb}^{9-x}$$

where C_9^x is the binomial coefficient

$$\left(\frac{9!}{x!(9-x)!}\right)$$

and p_{Cd} and p_{Pb} represent the atomic fractions of Cd and Pb, respectively. Assuming that the first metallic neighbours primarily determine the shielding of the phosphorus nucleus, one therefore expects essentially ten different ^{31}P chemical shifts.

With the oversimplified assumption of regular ^{31}P deshielding by increasing the number x of Cd atoms in the immediate environment of the phosphorus nucleus, the ^{31}P NMR MAS spectrum should present a maximum of ten isotropic signals with an interline separation of approximately (12.2 + 0.7)/9 ppm, i.e. 1.4 ppm (240 Hz at 9.4 T). The relative intensity of each signal is proportional to the probability of each environment. Actually, as shown in Figure 5 where it is evident that P, O1, O2, and three M2 atoms lie in the mirror plane, six types of metal atoms have to be considered and this can affect the shielding of the P nucleus in different ways, that is:

− in the mirror plane, $M_2(O_1)$, $M_2(O_2)$ and $M_2(O_3, O_3)$

− out of the mirror plane, $M_1(O_1)$, $M_1(O_2)$ and $M_2(O_3)$

Furthermore, for a given $[PCd_xPb_{(9-x)}]$ group, the ^{31}P chemical shift is also slightly affected by more remote metallic substituents.

Both these effects, which act as a perturbation of the dominant "nearest-neighbour effect" should, at best, lead to some broadening of the isotropic signal of the $[PCd_xPb_{(9-x)}]$ group with respect to those of the "pure" $[PPb_9]$ and $[PCd_9]$ groups (maximum broadening for the

most disordered cases [PCd_5Pb_4] and [PCd_4Pb_5]). The spectrum of a mixed lead−cadmium hydroxyapatite should therefore appear as a succession of nearly regularly spaced signals between $\delta = -0.7$ and $+12.2$, the most intense signal shifting progressively to higher frequencies by progressive replacement of lead by cadmium. Such types of solid-state MAS spectra were recently observed by ^{207}Pb NMR spectroscopy for solid solutions of lead−strontium nitrates.[19]

If the line width of the individual lines exceeds the chemical shift difference (due to both homogeneous and heterogeneous line broadening), the different signals are no longer resolved and the isotropic resonances should appear as a unique band, eventually with shoulders. The position of this band should shift to higher frequencies when increasing the cadmium content and its width should reach a maximum for an equal content of cadmium and lead. It is what is actually observed with the samples Cd20 and Cd30, for which the isotropic signal ($\Delta\nu_{1/2} \approx 1$ kHz) moves slightly from $\delta = 1.8$ to 1.9, but the spectra for the samples with lower Cd content cannot be explained in the frame of these assumptions.

Actually, the spectra of these mixed phases consist of two isotropic resonances at approximately the same positions [$\delta \approx -1.0$ (narrow) and $\delta \approx +1.0$ (broad)]. The relative intensity of both signals, obtained from line-fitting analysis, amounts to approximately 1:1 for Cd5 and approximately 1:3 for the Cd10 sample (Table 4). Although the overall line width is significantly larger for the latter ($\Delta\nu_{1/2} \approx 800$ Hz) than for the former ($\Delta\nu_{1/2} \approx 600$ Hz), no additional signal could be detected on the high frequency part of the isotropic band for the Cd10 sample. Therefore one must assume that identical $PPb_{(9-x)}Cd_x$ groups are present in both mixed phases, but with different concentrations. Let us return to the results of the Rietveld calculation: it has been demonstrated that cadmium atoms are preferentially located at site **1**. At low cadmium contents, Cd is almost exclusively at site **1**, as confirmed by crystallographic analysis (Table 2).

Furthermore, in manganese-substituted fluorapatites, Suitch et al.[20] showed that one Mn^{2+} ion at site **1** per unit cell distorts the phosphate tetrahedron in such a way that it hinders the fixation of another Mn^{2+} at both sites **1** and **2**, leading to the partial segregation of the Mn^{2+} ions in one of the four channels of the apatitic cell. This situation can also be anticipated in the present case of Pb−Cd apatites.

For an amount of 5% Cd, only one out of eight sites **1** are occupied by a Cd^{2+} ion: That means that only one out of every two unit cells contains a Cd^{2+} ion. Then two different environments for the phosphate group are equally probable, that is PPb_9 and $PCdPb_8$; or when considering only sites **1** in the unit cell (labelled as $_{S1}$): **A** = $[P(Pb_4)_{S1}]$ and **B** = $[P(CdPb_3)_{S1}]$ (see Figure 6), where **A** would give the narrow isotropic signal at $\delta = -1.0$ and **B** the relatively broad signal at $\delta = +1.0$. Distortion of the groups **B** with respect to **A** is apparent from the higher chemical-shift anisotropy of the corresponding NMR signal, leading to a relatively higher intensity of their spinning side bands at either rotor speeds (see Figure 3a).

For the manganese-substituted fluroapatites containing 5 atom-% Mn, Suitch et al.[20] observed two distinct IR stretching $\nu_1(PO_4)$ bands, which they assigned similarly to the two kinds of phosphate, with or without an interaction with a Mn^{2+} cation. For higher manganese content, Suitch et al.[20] observed the progressive disappearance of the IR band assigned to the phosphate group not interacting with an Mn^{2+} cation: they suggested that for the composition [$MnCa_9(PO_4)_6F_2$], there is strictly one Mn atom per unit cell, that is a regular arrangement of Mn^{2+} alternated with Ca^{2+} cations at one site **1** channel or, considering the P environment, there is one unique group $P(Ca_3Mn)_{S1}$.

A similar situation in Cd10 would lead to an NMR spectrum with a unique isotropic resonance at approximately $\delta = +1.0$ (due to group **B**). Actually, the NMR spectrum exhibits two resonances at $\delta = -1.0$ and $+1.0$. In agreement with the results obtained for Cd5, the two resonances could be assigned to a group **A** and to a group **B**. However, taking into account the stoichiometry of the sample, it is necessary to postulate the presence of a third group **C** containing two cadmium atoms at site **1,** with an **A/B/C** ratio of 0.25:0.5:0.25. This hypothesis would also justify the relative amounts of the two NMR signals, provided that the shielding for the **C** group is almost the same as that for the **B** group (that is, the chemical shift increment when substituting the second Cd^{2+} ion is smaller than that due to the first Cd^{2+} cation). The presence of **C** groups, with partial clustering of cadmium atoms in Cd_2 pairs, would explain

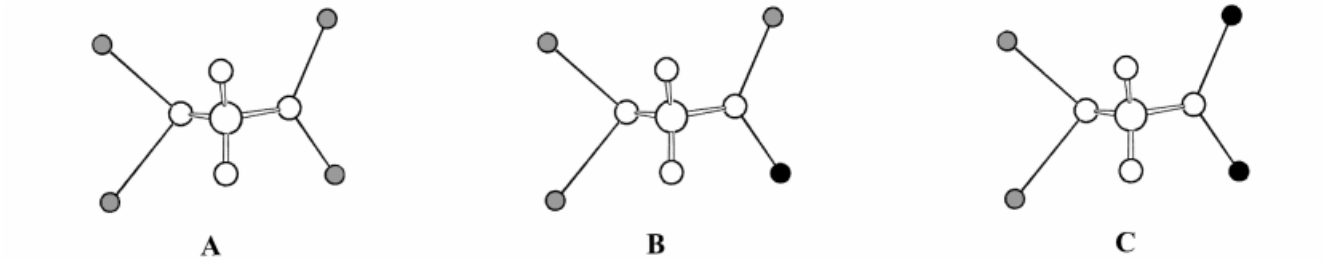

Figure 6. Phosphate group environments displaying three possible distributions of Pb (grey circles) and Cd (black circles) in site **1**

the pronounced phosphate distortion of the samples at low Cd content.

Conclusions

The results of this paper indicate that CdHA and PbHA exhibit only a limited range of solubility: cadmium can substitute lead up to 30 atom-%, whereas lead seems to avoid the incorporation into CdHA. Cadmium ions display a clear preference for site **1** of the apatite structure, in agreement with the shorter metal−metal distances at this site than at site **2**. When the cadmium content is increased, part of the substituent cations begin to fill site **2**, so that at the maximum degree of substitution, two of the four metal ions at site **1** are Cd, whereas only one of the six metal ions in the equilateral triangles characteristic of site **2** is Cd. The preference of cadmium for site **1** is responsible for the observed significant shift of the OH group towards the plane of the site **2** metals, as shown by its increase when the cadmium content at site **1** is increased. Furthermore, the presence of a relatively low amount of cadmium at site **1** induces a limited, but appreciable distortion of the phosphate tetrahedra that might be due to the presence of two different environments for the phosphate group, in agreement with the results of NMR spectroscopic analysis.

Experimental Section

General: Cadmium−lead hydroxyapatites were synthesized in aqueous systems by a double decomposition method,[6,7] starting from solutions containing 5, 10, 20, 30, 40, 50, 60 atom-% Cd, where atom-% = [Cd/Cd + Pb] × 100. The samples obtained are labeled as Cd%, where % is the amount of Cd^{2+} ions in the solution. − Stoichiometric quantities of cadmium nitrate and lead acetate (0.05 M solution A) and disodium hydrogen phosphate (0.03 M, solution B) were prepared separately in distilled water. The (Cd + Pb)/P molar ratio was adjusted to be the stoichiometric one (1.67); each solution was stirred under nitrogen. Solution A was added to solution B, maintained at 100 °C under nitrogen to improve the homogeneity of the precipitate, and to prevent the formation of carbonated apatites. The precipitate was allowed to be in contact with the mother solution for 2 h, then filtered and washed with hot distilled water. An aqueous solution of ammonia was then added in order to maintain the pH value at about 11 during the maturation (3 h) at 100 °C. The precipitate was then filtered and dried at 110 °C for 24 h. − The XRD data were collected with a Philips PW 1710 diffractometer using a graphite monochromator. The step range was from 5 to 95°(2θ), with a counting time of 10 s for each step and a step width of 0.03°. − ^{31}P MAS NMR spectra were obtained at room temperature with a Bruker MSL400 spectrometer (9.4 T) operating at 162 MHz, using a 4-mm MAS Doty probe. − Magic angle spinning (MAS) spectra were obtained with spinning rates up to 5 kHz, using single-pulse excitation. Chemical shifts are reported relative to 85% aqueous orthophosphoric acid H_3PO_4 (δ= 0).

Structural Analysis: The full pattern refinements were carried out by means of the Rietveld method using the DBWS-9411 program.[21,22] − The space group ($P6_3/m$, no. 176) and the atomic positions of the lead hydroxyapatite structure[12] were used as the starting set in the refinement procedure. The X-ray scattering factors for Cd^{2+}, Pb^{2+}, O^- ions and for the P atom were used. A third-order polynomial was employed to assimilate the background while the peaks were fitted by using a pseudo-Voigt function. The halfwidth of the diffraction peaks as a function of 2θ was evaluated by the Caglioti equation.[23] In the first cycles, the scale factor and the background coefficients were refined. Successively, the profile parameters (peak widths and their dependence on 2θ, true 2θ zero, Lorentzian fraction) and the lattice parameters were allowed to vary too. Finally, the occupancy factors (O.F.) were refined and the cation substitution was tested. − No constraint was imposed on the overall cadmium content. The two metal sites were imposed to be fully and complementarily occupied by lead and cadmium. The occupancy factors of O and P were assumed as constant, in agreement with the apatite stoichiometry. The fractional atomic coordinates were refined, starting from the atomic positions of the two metals. No attempt was made to distinguish the position of Pb atoms from that of the substituting Cd atoms. The same thermal factors (t.f.) were used for Cd and Pb atoms; the individual t.f. values were kept constant but an overall thermal parameter was refined. In the last refinement cycles, optimizing 28 variables (structural and nonstructural parameters) simultaneously tested the possible preferred orientations of the 001 reflections. All the nonstructural refined parameters are reported as Supporting Information and are available on the WWW under http://www.wiley-vch.de/home/eurjic or from the author. − Further details of the crystal-structure investigations may be obtained from the Fachinformationszentrum Karlsruhe, 76344 Eggenstein-Leopoldshafen, Germany, on quoting the depository numbers CSD-411418 to -411421.

Acknowledgments

We greatly acknowledge financial support from MURST (Italy), the University of Bologna (Funds for Selected Topics), the Direction Générale de la Recherche Scientifique et Technique (Tunisia) and the Centre National de la Recherche Scientifique (France).

[1] *CRC Handbook of Bioactive Ceramics*, vol. II ("Calcium Phosphates and Hydroxyapatite Ceramics") (Eds.: T. Yamamuro, L. L. Hench, J. Wilson), CRC Press, Boca Raton, **1990.**
[2] J. C. Elliott, *Structure and Chemistry of the Apatites and Other Calcium Orthophosphates*, Elsevier Sci., The Netherlands, **1994.**
[3] A. Bigi, E. Foresti, M. Gandolfi, M. Gazzano, N. Roveri, *J. Inorg. Biochem.* **1995**, *58*, 49−58.
[4] I. Mayer, H. Cohen, J. C. Voegel, F. J. G. Cuisinier, *J. Cryst. Growth* **1997**, *172*, 219−225.
[5] J. Christoffersen, M. R. Christoffersen, N. Kolthoff, O. Bärenholdt, *Bone* **1997**, *20*, 47−54.
[6] A. Bigi, M. Gazzano, A. Ripamonti, E. Foresti, N. Roveri, *J. Chem. Soc., Dalton Trans.* **1986**, 241−244.
[7] A. Bigi, G. Filini, E. Foresti, M. Gazzano, A. Ripamonti, N. Roveri, *J. Inorg. Biochem.* **1993**, *49*, 69−78.
[8] H. Heijiligers, F. C. M. Driessens, R. M. H. Verbeck, *Calcif. Tissue Int.* **1979**, *29*, 127−131.
[9] A. Bigi, A. Ripamonti, S. Brückner, M. Gazzano, N. Roveri, S. A. Thomas, *Acta Crystallogr.* **1989**, *B45*, 247−251.
[10] M. T. Kay, R. A. Young, S. A. Posner, *Nature* **1964**, *204*, 1050−1052.
[11] M. Hata, K. Okada, S. Iwai, M. Akao, H. Aoki, *Acta Crystallogr.* **1978**, *B34*, 3062−3064.
[12] S. Brückner, G. Lusvardi, L. Menabue, M. Saladini, *Inorg. Chim. Acta* **1995**, *236*, 209−212.
[13] A. Bigi, M. Gandolfi, M. Gazzano, A. Ripamonti, N. Roveri, A. Thomas, *J. Chem. Soc., Dalton Trans.* **1991**, 2883−2886.
[14] W. H. Baur, *Acta. Crystallogr.* **1974**, *B30*, 1195−1215.
[15] M. T. Weller, G. Wong, *J. Chem. Soc., Chem. Commun.* **1988**, 1103−1104.

[16] J. P. Yesinowski, *J. Am. Chem. Soc.* **1981**, *103*, 6266−6267.
[17] B. Badraoui, M. Debbabi, R. Thouvenot, *C. R. Hebd. Acad. Sci., Ser. IIC* **2000**, *3*, 107−112.
[18] B. Badraoui, M. Debbabi, R. Thouvenot, unpublished results.
[19] Y.-S. Kye, G. S. Harbison, *Inorg. Chem.* **1998**, *37*, 6030−6031.
[20] P. R. Suitch, J. L. LaCout, A. Hewat, R. A. Young, *Acta Crystallogr.* **1985**, *B41*, 173−179.
[21] M. Rietveld, *J. Appl. Crystallogr.* **1969**, *2*, 65−71.
[22] R. A. Young, A. Sakthivel, T. S. Moss, C. O. Paiva−Santos, *J. Appl. Crystallogr.* **1995**, *28*, 366−367.
[23] G. Caglioti, A. Paoletti, F. P. Ricci, *Nucl. Instrum.* **1958**, *3*, 223−228.

Received August 4, 2000
[I00306]